

# The phenotype-o-mat: A flexible tool for collecting visual phenotypes

**We've developed an easy-to-assemble apparatus and software for the automated collection of visible biological phenotypes such as growth, macroscopic morphology, motion, reflectance, and fluorescence.**

Version 2, published Mar 13, 2025. Originally published Apr 23, 2024.

 Arcadia Science

DOI: 10.57844/arcadia-112f-5023

## Purpose

Many projects at Arcadia require us to collect visual phenotypes from Petri dishes or multiwell plates, but the existing tools for this are often cumbersome, expensive, and difficult to adapt to new protocols. We therefore created an easily extensible imaging system by combining a low-cost but high-quality camera, a microcontroller-mediated multi-wavelength illumination system, and a software package for writing data acquisition protocols.

We're sharing the information necessary to assemble the "phenotype-o-mat," as well as the software required to operate it and example "protocols" written with that software. This pub may be helpful to anyone interested in collecting visual biological phenotypes.

- This pub is part of the **project**, "[Genetics: Decoding evolutionary drivers across biology.](#)" Visit the project narrative for more background and context.
- All associated **code**, including example analysis scripts, is available [in this GitHub repository](#).
- All the **data** we collected in the example assays, including raw image and video files, are available on [Zenodo](#).
- An accompanying **protocol** for [assembling your own phenotype-o-mat](#) is available at protocols.io.

# The strategy

As part of the platform effort "Genetics: Decoding evolutionary drivers across biology," we've created a hybrid population of the photosynthetic algae *Chlamydomonas* by crossing *C. reinhardtii* and *C. smithii*. Motivated by some of our previous work [1][2] suggesting analysis of many high-dimensional phenotypes will aid in genotype-phenotype mapping, we're conducting high-throughput genotype and phenotype analysis on this hybrid population. Accordingly, we sought to create a flexible and inexpensive tool for collecting a broad range of phenotypes (e.g. growth rate, colony morphology, chlorophyll fluorescence) from these strains. The design would need to be easy to program, extensible, and potentially useful for other projects at Arcadia. Our solution, described in this pub and a companion protocol, is a simple imaging device with trans-illumination, incident illumination of multiple wavelengths, an optical filter slider for fluorescence assays, and complementary software intended to make programming assays on the device easy.

## The problem

For many studies, collecting biological measurements is a bottleneck. Assays often require expensive specialized equipment and experimenter supervision, and they can be difficult to adapt to new biological questions.

## Our solution

We developed an inexpensive and easily extensible tool for the automated collection of image-based biological measurements. The "phenotype-o-mat" (Figure 1) consists of a quantitative camera, white-light transmission illumination, several wavelengths of incident illumination, a filter slider, and software infrastructure for programming the camera and illumination system to conduct assays such as cellular growth curves, reflectance, fluorescence, videos, and time series.

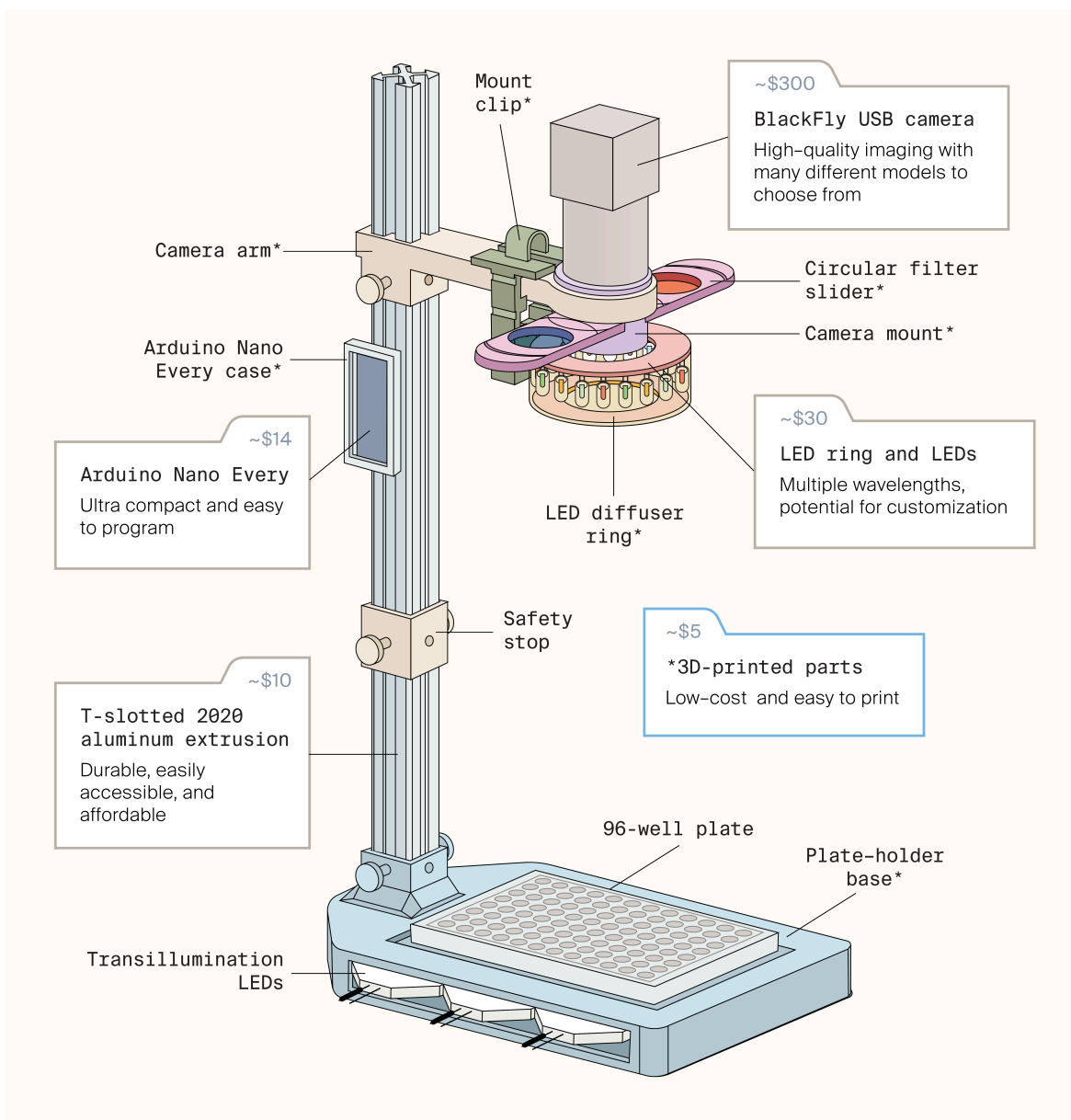


Figure 1. **Schematic of the phenotype-o-mat.**

Approximate costs of individual parts are noted. Components with an asterisk (\*) are 3D-printed.

## Why is this useful?

The phenotype-o-mat allows the collection of image data including reflectance in four wavelengths, fluorescence, cell density, colony morphology, and small animal behavior (e.g. nematodes or flies). It can collect data in densely sampled videos (up to ~1,000 frames per second) or in arbitrarily long time-lapse imaging sessions. The camera is very sensitive and provides quantitative data. For people in need of different functionality (e.g., different frame rates, resolutions, pixel sizes, quantum efficiencies, or polarization sensitivities), there are other cameras

available from the same manufacturer that are compatible with the same software. For fluorescence assays, we add a filter to the front of the camera. Inexpensive filters for many wavelengths are widely available, allowing easy extension of the system's functionality.

Alternatives to this system such as plate readers or multi-wavelength imagers are expensive and less flexible. For example, adding a new wavelength of incident illumination to the phenotype-o-mat is as simple as ordering a few more light-emitting diodes. Adding wavelengths to a plate reader or imager could cost thousands of dollars or may simply be impossible.

## The resource

The phenotype-o-mat is a basic imaging system that you can build yourself from a mix of 3D-printed and commercially available, inexpensive parts ([Figure 2](#)). For detailed, step-by-step instructions on how to assemble the device yourself, check out our [accompanying protocol](#). If you run into any issues, please comment on the protocol or the pub and we're happy to talk you through it.

This section provides an overview of the components required for the device, a quick summary of how to assemble it, some of the decision-making behind its design, and two example assays that it can perform.

All associated **code**, including example analysis scripts, is available on [GitHub](#) (DOI: [10.5281/zenodo.11050006](#)). **Data** collected in our example assays, including raw image and video files, are available on [Zenodo](#) (DOI: [10.5281/zenodo.11043291](#)).

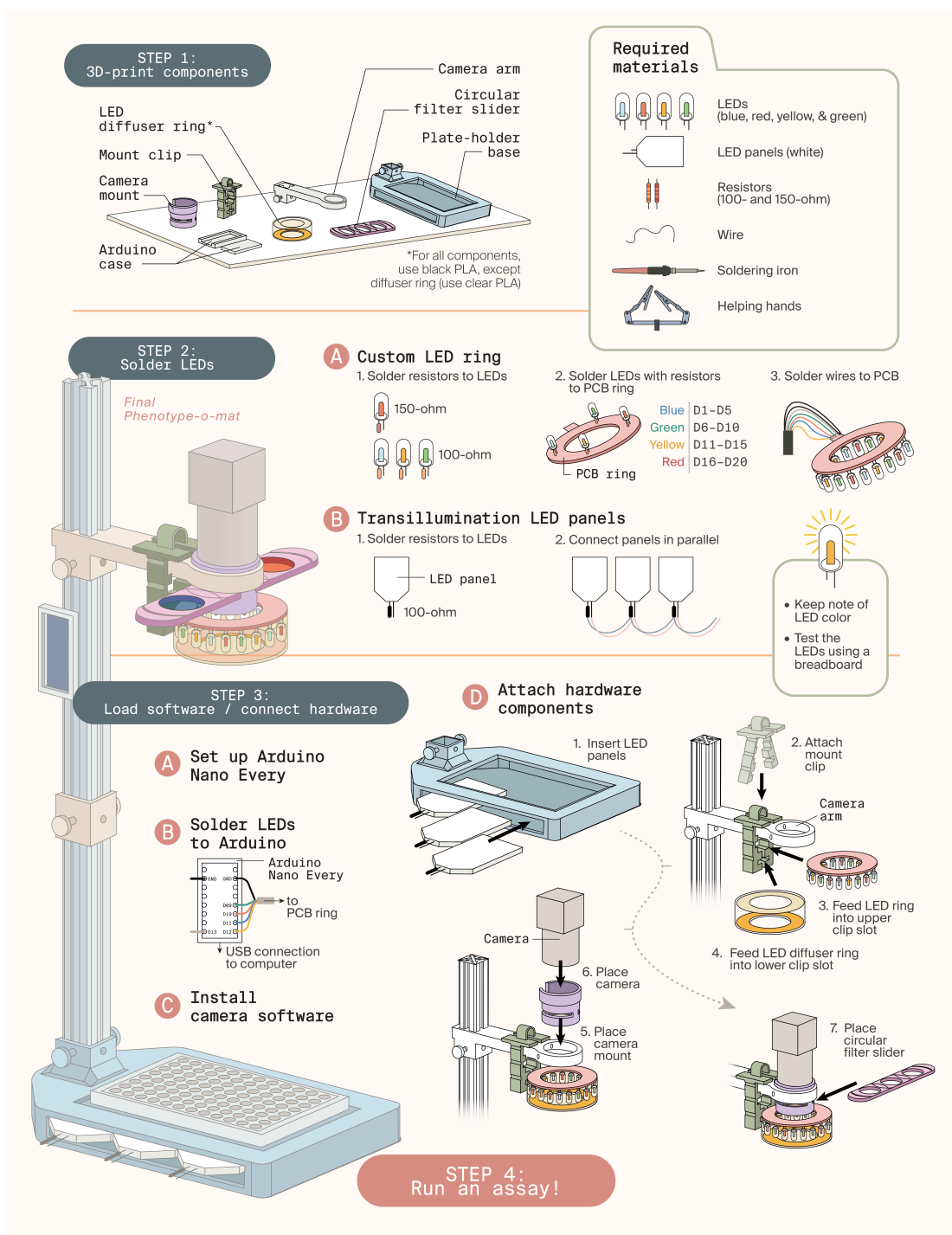


Figure 2. **Assembling the phenotype-o-mat.**

Overview of the required components and their assembly. For full details, see our [assembly instructions on protocols.io](https://protocols.io).

## Components

To develop our imaging system, we first identified cameras that would be quantitative and flexible. We chose the Blackfly S line of cameras from Teledyne. There are many types of imaging chips available in the Blackfly S format, enabling a researcher to optimize for their individual needs. Some cameras have high

frame rates, high quantum efficiency, high resolution, low read noise, or specialized features such as simultaneously imaging different polarizations. Furthermore, they all interface with the same software development kit, and so will all be compatible with the software we've developed.

We chose the Arduino line of microcontrollers to interface with the illumination system and other possible future peripherals, like an automated filter wheel or a vibrational stimulator for the samples. The Arduino microcontroller ecosystem is well-established and supported. The controllers themselves are inexpensive, easy to program, and have a wide range of functionality.

With the basic components established, we then decided on a core set of imaging functionalities for the phenotype-o-mat: transillumination, incident illumination of four wavelengths, and the ability to use filters for fluorescence assays.

## Assembly

A **components list** and **comprehensive instructions** on the assembly of the phenotype-o-mat is available on [protocols.io](https://protocols.io).

Briefly, you begin by 3D-printing the physical components. You can also order these [here](#). Next, you'll add threaded inserts to the plate-holder base and camera arm with the help of a soldering iron. To assemble the illumination ring, you solder current-modulating resistors to each light-emitting diode, then solder these diodes to the printed circuit board for the illumination ring. Next, solder wires connecting the illumination ring to the microcontroller. You go through a similar process for the transillumination panels. You then assemble the physical apparatus by: 1) fitting the 20 mm × 20 mm aluminum extrusion into the plate-holder base and securing it by adding thumb screws into the threaded inserts, 2) inserting the transillumination LED panels into the base, 3) adding the camera arm to the extrusion and securing it with thumbscrews, 4) attaching the illumination mount and the LED ring and diffuser, and 5) adding the camera mount and the camera itself. After physical assembly, you'll install the firmware on the microcontroller and the imaging software.

## Example assays and data analysis

In this section, we provide some example assays we've conducted with the phenotype-o-mat, providing a sense of the breadth of its utility. In our first example, we quantify the reflectance of four different wavelengths of light by two *Chlamydomonas* species: *C. reinhardtii* and *C. smithii*. In this assay, the species are arrayed in 96-well format on solid media plates. In the second example, we measure the decay in chlorophyll fluorescence in these same two species streaked onto Petri dishes\*. This fluorescence decay is induced when dark-adapted organisms are exposed to light for an extended period. The decay captures biophysical and biochemical responses that allow the organism to adapt to continuous light exposure [3][4].

You can find **analysis scripts** that generated the technical components of these figures on [GitHub](#), and the **data** are available on [Zenodo](#).

### Multi-wavelength reflectance and colony size

Spectral reflectance patterns have been used to identify plant and microbe species [5][6]. This has been a powerful method in the remote sensing field, but little used to evaluate the phenotypes of different strains in a laboratory setting. The phenotype-o-mat can evaluate reflectance in four wavelengths of light: 460 nm, 535 nm, 590 nm, and 670 nm.

As part of the platform effort "[Genetics: Decoding evolutionary drivers across biology](#)," we created a hybrid population of the photosynthetic algae *Chlamydomonas* by crossing *C. reinhardtii* and *C. smithii*. We've subjected this population to phenotypic and genetic analysis with high-throughput methods and have spent significant effort to characterize the phenotypes of the two parental species [7].

In this assay, we sought to determine if the two parental strains yielded differing spectral reflectance patterns. If we were to find variation, we would then use these patterns as a complex phenotype in our *Chlamydomonas* hybrid population.

We grew *Chlamydomonas* colonies on TAP media [8] at room temperature and 24-hour illumination arrayed in 96-well format on a single-well microtiter plate. We positioned this microtiter plate in the plate holder at the base of the phenotype-omat. We then covered the imaging system with a dark box and ran a script that conducted the following steps:

1. Turn on the transillumination light source.
2. Acquire a single image to allow colony segmentation and turn off the transillumination.
3. Turn on one of the four incident illumination wavelengths available.
4. Image the colonies and turn off the incident illumination.
5. Repeat starting at step three until we've imaged colony reflectance at all wavelengths.

The **script** implementing this experimental regimen is available on [GitHub](#).

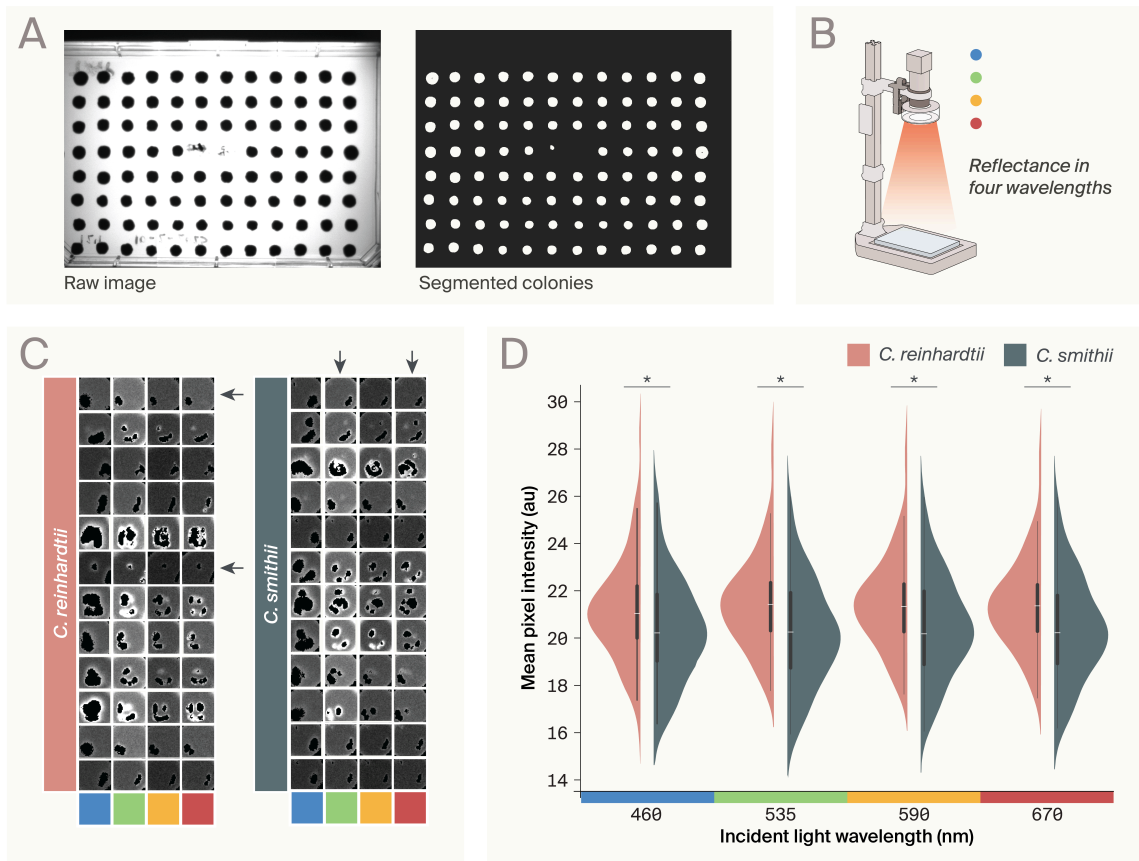


Figure 3. **Spectral reflectance data we collected with the phenotype-o-mat show that *C. reinhardtii* reflects more light than *C. smithii*.**

(A) A raw image from the phenotype-o-mat (left) and a processed version in which colony segmentation is indicated by shading (right).

(B) Schematic depicting multi-wavelength incident illumination, the setup used to collect the data in C and D.

(C) Four images (one for each wavelength, left to right) for each of 12 representative individual colonies of each species. Colors below columns indicate wavelength (blue = 460 nm, green = 535 nm, yellow = 590 nm, and red = 670 nm). Horizontal arrows indicate examples with variation in reflectance between colonies and vertical arrows indicate examples with variation across wavelengths.

(D) Mean pixel intensities for both *Chlamydomonas* species we tested across four different wavelengths of incident light. au = arbitrary units. An asterisk (\*) indicates a significant difference ( $p < 0.01$ , two-tailed  $t$ -test).

Analyses of data we collected via this approach for *C. reinhardtii* and *C. smithii* are shown in [Figure 3](#). We used transillumination images of single-well microtiter plates where colonies are organized in 96-well format ([Figure 3](#), A, left) to identify and segment individual colonies ([Figure 3](#), A, right).

We then propagated these segmentations across each of the four incident illumination images of these same microtiter plates. Representative individual

colonies for each of these four images (illumination wavelengths indicated at the top of each column) for both species are shown in [Figure 3](#), B. In these images, surface reflectance (glare) is shown in black. We noticed positional effects, likely from uneven illumination, in reflectance where individual wells exhibited more or less reflected light across all wavelengths (compare horizontal arrows), which will contribute structured noise to our data. But, we also noted that there was consistent reflectance of specific wavelengths across individual colonies (compare vertical arrows) likely indicating that, for any given species, there is consistent variation of reflectance across wavelengths independent of well position.

While we could statistically control for the types of variation caused by colony position, for this initial work we took an agnostic approach and simply compared the difference in reflectance between *C. reinhardtii* and *C. smithii* without controlling for possible confounding variables. This analysis is shown in [Figure 3](#), C. We found that, for all wavelengths, *C. reinhardtii* (red, left) reflected more light than *C. smithii* (green, right,  $p < 0.01$ , two-tailed *t*-test). Likely, these effects would be further accentuated and resolved if we controlled for colony position to account for the uneven illumination.

## **Chlorophyll fluorescence decay**

In dark-adapted plants and photosynthetic algae, exposure to light induces an increase in fluorescent light emitted by chlorophyll A contained in photosystem II [3][4]. The increase in light emission and the subsequent decay that occurs with sustained light exposure contains characteristic indicators of the photosynthetic process, including the efficiency of photosynthesis [9] as well as the photochemical [10] and non-photochemical [11] mechanisms that protect photosynthetic organisms from over-exposure to light. Furthermore, researchers have used both fluorescence induction and decay to guide genetic screens for genes involved in photosynthesis [12].

We sought to develop an assay for the phenotype-o-mat that would allow us to efficiently assess chlorophyll fluorescence decay such that we could analyze the slower components of fluorescence decay in our *Chlamydomonas* hybrid population described above.

For this assay, we positioned a 650 nm longpass filter in the light path, allowing only the fluorescence (mostly from chlorophyll) at wavelengths above 650 nm to access the camera. We placed a single-well microtiter plate containing 96 *Chlamydomonas* colonies growing on TAP media into the plate holder at the base of the phenotype-o-mat. We then covered the imaging system with a dark box and ran a script that conducted the following steps:

1. Wait 15 min for the *Chlamydomonas* to dark-adapt [12].
2. Turn on the 460 nm incident illumination LED.
3. Once a minute for 20 min, collect 5 s of video at 260 Hz.

The **script** implementing this experimental regimen is available on [GitHub](#).

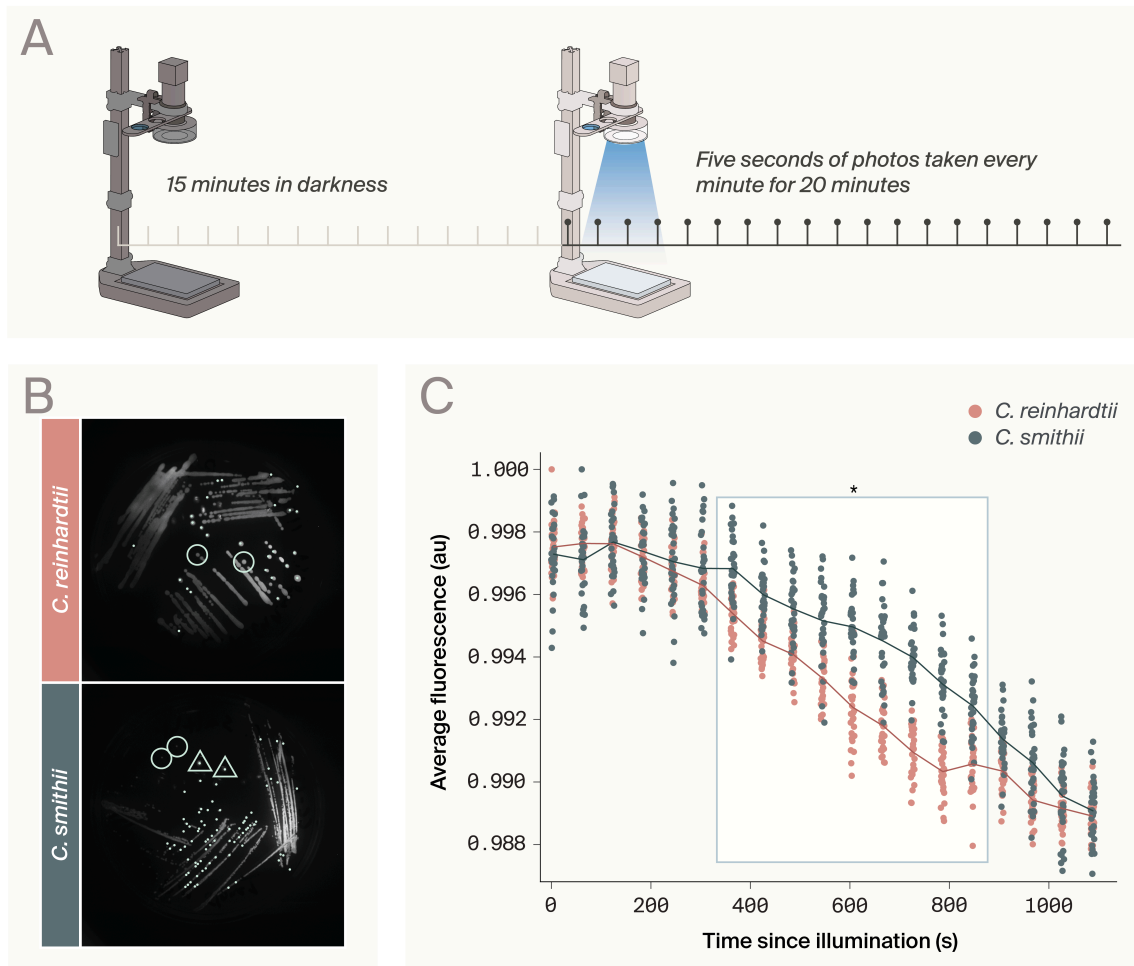


Figure 4. **Chlorophyll fluorescence decay data we collected with the phenotype-o-mat show that *C. reinhardtii* and *C. smithii* differ in their rate and intensity of decay.**

(A) Schematic of the experimental protocol used to collect the data in C.

(B) Segmented images of *C. smithii*, (top) and *C. reinhardtii* (bottom). Segmented colonies passing filters are indicated by dots. Clearly separated colonies that our process failed to identify are shown in circles and light reflections incorrectly classified as colonies are shown in triangles.

(C) Average decay trajectories for *C. smithii* colonies (gray) and *C. reinhardtii* colonies (salmon). Time points are the average fluorescence intensity of all segmented colonies at each acquired time point. The white box with an asterisk (\*) contains time points that differ significantly between the two species ( $p < 0.01$ , two-tailed  $t$ -test).

We then calculated the average emitted light intensity for each colony at each time point (Figure 4). For this experiment, and in contrast to the reflectance data, we imaged *C. reinhardtii* (Figure 4, A, top) and *C. smithii* (Figure 4, A, bottom) as individual colonies streaked on TAP media in Petri dishes. To identify colonies, we segmented the first image from a series (Figure 4, A, first column) based on fluorescence intensity and filtered based on aspect ratio and colony size. Colonies passing filtration for each species are indicated in red in Figure 4, A, second column. This process was imperfect — several well-separated individual colonies

(examples indicated by circles in [Figure 4](#), B) were not identified by this approach and, in some instances, reflectance from the media was classified as colonies (examples indicated by triangles in [Figure 4](#), B). Nonetheless, using this acquisition and analysis, both *C. reinhardtii* and *C. smithii* have a fluorescence trajectory consistent with previous findings, where there's an initial spike in emission followed by a slow decay ([Figure 4](#), B) [3][4]. However, the two species significantly differed in the rate and complexity of this decay ([Figure 4](#), B, significant differences between time points indicated by bar,  $p < 0.01$ , two-tailed *t*-test). This result suggests that this approach to quantifying chlorophyll fluorescence decay is useful in categorizing individual species and that it will be interesting to investigate the segregation of this phenotype in our *Chlamydomonas* diversity population.

All **analysis scripts** that generated these figures are available on [GitHub](#), and the **data** are available on [Zenodo](#).

## Next steps

The phenotype-o-mat is intended as an extensible system and we plan to continue expanding its functionality as new needs arise. For example, these analyses used a version of the apparatus with a commercially available imaging [stand](#), while our [newer version](#) contains a more flexible 3D-printed imaging stand and produces similar data.

While we don't plan to modify the device in the immediate future, we'll share updates when they come and we hope you'll try developing assays for your own research. If you have questions for us or thoughts to inspire other readers, please comment on the pub! We'd especially love to hear from you if you try building a phenotype-o-mat and have any feedback.

---

## Contributors (A-Z)

- **Audrey Bell**: Visualization
- **Ben Braverman**: Methodology, Validation

- **Megan L. Hochstrasser:** Editing
- **Cameron Dale MacQuarrie:** Validation
- **David G. Mets:** Conceptualization, Formal Analysis, Investigation, Methodology, Software, Visualization, Writing
- **Taylor Reiter:** Validation
- **Ryan York:** Supervision

## References

1. Avasthi P, Mets DG, York R. (2023). Harnessing genotype-phenotype nonlinearity to accelerate biological prediction. <https://doi.org/10.57844/arcadia-5953-995f>
2. Mets DG, York R. (2023). Applying information theory to genetics can better explain biological phenomena. <https://doi.org/10.57844/arcadia-53f4-da1a>
3. Kautsky H, Hirsch A. (1931). Neue Versuche zur Kohlenstoffassimilation. <https://doi.org/10.1007/bf01516164>
4. Kalaji HM, Schansker G, Brestic M, Bussotti F, Calatayud A, Ferroni L, Goltsev V, Guidi L, Jajoo A, Li P, Losciale P, Mishra VK, Misra AN, Nebauer SG, Pancaldi S, Penella C, Pollastrini M, Suresh K, Tambussi E, Yannicari M, Zivcak M, Cetner MD, Samborska IA, Stirbet A, Olsovska K, Kunderlikova K, Shelonzek H, Rusinowski S, Bąba W. (2016). Frequently asked questions about chlorophyll fluorescence, the sequel. <https://doi.org/10.1007/s11120-016-0318-y>
5. Bahrami M, Mobasheri MR. (2020). Plant species determination by coding leaf reflectance spectrum and its derivatives. <https://doi.org/10.1080/22797254.2020.1816501>
6. Olmedo-Masat OM, Raffo MP, Rodríguez-Pérez D, Arijón M, Sánchez-Carnero N. (2020). How Far Can We Classify Macroalgae Remotely? An Example Using a New Spectral Library of Species from the South West Atlantic (Argentine Patagonia). <https://doi.org/10.3390/rs12233870>
7. Avasthi P, Braverman B, Essock-Burns T, Garcia III G, MacQuarrie CD, Matus DQ, Mets DG, York R. (2023). Phenotypic differences between interfertile *Chlamydomonas* species. <https://doi.org/10.57844/arcadia-35f0-3e16>
8. (2023). The *Chlamydomonas* Sourcebook. <https://doi.org/10.1016/c2019-0-02810-5>

9. Baker NR. (2008). Chlorophyll Fluorescence: A Probe of Photosynthesis In Vivo. <https://doi.org/10.1146/annurev.arplant.59.032607.092759>
10. Ruban AV. (2016). Nonphotochemical Chlorophyll Fluorescence Quenching: Mechanism and Effectiveness in Protecting Plants from Photodamage. <https://doi.org/10.1104/pp.15.01935>
11. Terjung F, Maier K. (1998). Nonphotochemical Quenching of Chlorophyll Fluorescence in Higher Plant Leaves Studied by Delayed Fluorescence Decay Measurements. <https://doi.org/10.1515/znc-1998-1-207>
12. Ogawa T, Sonoike K. (2021). Screening of mutants using chlorophyll fluorescence. <https://doi.org/10.1007/s10265-021-01276-6>